Published in final edited form as:

Circ Res. 2016 November 11; 119(11): 1215–1225. doi:10.1161/CIRCRESAHA.116.309598.

CD45 Expression in Mitral Valve Endothelial Cells After Myocardial Infarction

Joyce Bischoff[1], **Guillem Casanovas**[1], **Jill Wylie-Sears**[1], **Dae Hee Kim**[2,3], **Philipp E. Bartko**[2], **J. Luis Guerrero**[2], **Jacob P. Dal-Bianco**[2], **Jonathan Beaudoin**[2], **Michael L. Garcia**[2], **Suzanne M. Sullivan**[2], **Margo M. Seybolt**[2], **Brittan A. Morris**[2], **Joshua Keegan**[4], **Whitney S. Irvin**[4], **Elena Aikawa**[4], and **Robert A. Levine**[2]

[1]Vascular Biology Program and Department of Surgery, Boston Children's Hospital, Harvard Medical School, Boston, MA, USA

[2]Cardiac Ultrasound Laboratory, Massachusetts General Hospital, Harvard Medical School, Boston, MA, USA

[3]Division of Cardiology, Asan Medical Center, College of Medicine, University of Ulsan, Seoul, Korea

[4]Center for Excellence in Vascular Biology, Division of Cardiovascular Medicine, Brigham and Women's Hospital, Harvard Medical School, Boston, MA, USA

Abstract

Rationale—Ischemic mitral regurgitation (IMR), a complication after myocardial infarction (MI), induces adaptive mitral valve (MV) responses that may be initially beneficial, but eventually lead to leaflet fibrosis and MV dysfunction. We sought to examine the MV endothelial response and its potential contribution to IMR.

Objective—Endothelial, interstitial and hematopoietic cells in MVs from post-MI sheep were quantified. MV endothelial CD45, found post-MI, was analyzed in vitro.

Methods and Results—Ovine MVs, harvested 6 months after inferior MI (IMI), showed CD45, a protein tyrosine phosphatase, co-localized with von Willebrand factor, an endothelial marker. Flow cytometry of MV cells revealed significant increases in CD45-positive endothelial cells (VE-Cadherin+/CD45+/α-smooth muscle actin (SMA)+ and VE-cadherin+/CD45+/αSMA- cells) and possible fibrocytes (VE-Cadherin-/CD45+/ αSMA+) in IMI compared to sham-operated and normal sheep. CD45+ cells correlated with MV fibrosis and MR severity. VE-cadherin+/CD45+/αSMA+ cells suggested CD45 may be linked to endothelial-to-mesenchymal transition (EndMT). MV endothelial cells treated with TGFβ1 to induce EndMT expressed CD45 and fibrosis markers collagen 1 and 3 and TGFβ1–3, not observed in TGFβ1-treated arterial

Address correspondence to: Dr. Joyce Bischoff , Vascular Biology Program, Boston Children's Hospital, Boston, MA 02115, Tel: 617-919-2192, Fax: 617-730-0231, joyce.bischoff@childrens.harvard.edu.
J.B., G.C., and J.W-S. contributed equally to this manuscript.

DISCLOSURES
None.

endothelial cells. A CD45 protein tyrosine phosphatase inhibitor blocked induction of EndMT and fibrosis markers, and inhibited EndMT-associated migration of MV endothelial cells.

Conclusions—MV endothelial cells express CD45, both in vivo post-MI and in vitro in response to TGFβ1. A CD45 phosphatase inhibitor blocked hallmarks of EndMT in MV endothelial cells. These results point to a novel, functional requirement for CD45 phosphatase activity in EndMT. The contribution of CD45+ endothelial cells to MV adaptation and fibrosis post-MI warrants investigation.

Keywords

Mitral valve; mitral regurgitation; myocardial infarction; CD45; valve endothelial cells; endothelial-to-mesenchymal transition; endothelial cell differentiation; endothelial cell

INTRODUCTION

Ischemic mitral regurgitation (IMR) is a common complication after myocardial infarction (MI) that doubles mortality [1]. IMR is caused by left ventricular remodeling and dysfunction, which leads to papillary muscle displacement and tethering of the mitral valve (MV), restricting leaflet closure[1]. Tethered MVs adapt by increasing their surface area, but this adaptation is often insufficient and appears to result in stiff, fibrotic valves, which may ultimately contribute to increasing IMR [2–5].

Several cellular events occur in the IMR MV: MV endothelial cells (mitral VECs) undergo endothelial-to-mesenchymal transition (EndMT), MV interstitial cell (mitral VICs) are activated to become myofibroblasts that secrete and compact extracellular matrix, and there is evidence for valve neovascularization and leukocyte infiltration [2, 5–8]. Infiltrating macrophages and leukocytes release growth factors and cytokines, such as TGFβ family members, which can promote angiogenesis, collagen production and attraction of additional inflammatory cells, while transforming interstitial cells to myofibroblasts that also secrete growth factors and cytokines. Thus, TGFβ isoforms may also be produced endogenously by the MV cells [9,10, 11].

In this work we used an ovine inferior MI (IMI) model to study the MV endothelium in the context of valve growth and fibrosis in response to IMR. Immunohistochemistry and flow cytometry of MV leaflets from infarcted sheep revealed endothelial cells positive for the leukocyte marker/protein tyrosine phosphatase CD45. Flow cytometry further revealed CD45+/α-smooth muscle actin (α-SMA)+ cells which may be fibrocytes[12, 13] and CD45+ hematopoietic cells in the MV, all of which might contribute to development of fibrosis in IMR. Fibrocytes are circulating CD45+ myeloid cells that migrate into sites of inflammation or tissue injury and, under the influence of cytokines and TGFβ, transform into α-SMA+ myofibroblast-like cells[13] In vitro, CD45 was induced in several ovine mitral VEC clones by the fibrogenic factor TGFβ1, which potently induces endothelial-to-mesenchymal transition (EndMT) in these cells[14, 15]. Blocking CD45 protein tyrosine phosphatase activity pharmacologically inhibited expression of EndMT and fibrosis markers and EndMT-associated enhanced migration in mitral VEC. TGFβ did not induce CD45, EndMT or fibrosis markers or migration in ovine carotid artery endothelial cells (CAEC), indicating

specificity. Our findings uncover an unanticipated role for CD45 in TGFβ-stimulated EndMT and suggest that mitral VECs may be a source of fibrotic cells in IMR.

METHODS

Animal model

A total of 13 Dorsett hybrid sheep were analyzed. The IMI sheep (n=5) had ligation of their second and third obtuse marginal branches of the left circumflex coronary artery. Two- and 3-dimensional echocardiography was performed before MI and 30–60 minutes following MI. Six months post-MI, echocardiograms were repeated to assess MR and the animals euthanized and their MVs excised. The excised MV leaflet tissue was immediately submerged in a solution of 5% heat-inactivated fetal bovine serum (FBS), 4% Penicillin/Streptomycin/Amphotericin B, 1% L-Glutamine and 0.2% gentamycin sulfate in EBM-2 medium (Lonza Inc., GA, USA, #CC-3156), and kept on ice at 4°C until processed. MV from five (n=5) age and weight-matched sheep who underwent sham procedures (thoracotomy without infarction) were analyzed as controls. Echocardiographic measurements are shown in Online Table I. Three-dimensional (3D) echocardiographic analysis included LV end-systolic and end-diastolic volumes integrated from multiple rotated views derived from the full 3D dataset using Omni4D software; infarct size as endocardial surface area (ESA) measured at end diastole based on visualized wall motion hinge points; and total LV remodeling reflected by the increase in total LV ESA from immediately to 6 months post-MI[16–19]. In addition, mitral valves from normal sheep (n=3) were analyzed (Online Table I). Animals were monitored by qualified AAALAC-certified veterinary staff. These studies conform to National Institutions of Heath guidelines for animal care and received Institutional Animal Care Committee approval.

Immunohistochemistry

A portion of each excised MV was frozen in OCT compound (Sakura Finetek, Tokyo, Japan), sectioned and stained with primary mouse anti sheep CD45 antibody (AbD Serotec, NC, USA, cat# MCA2220GA) or anti-sheep CD14 (AbD Serotec, cat#MCA920GA) by the avidin-biotin-peroxidase method or by fluorescence double-labeling for von Willebrand Factor (vWF; DAKO, CA, USA, cat#, A0082) as described[20]. Masson Trichrome staining to assess collagen accumulation as an indication of fibrosis was performed as in previous studies[5, 8]

Flow cytometry

Ovine MVs were minced and digested for 30 minutes at 37°C with Liberase (Roche Diagnostics, IN, USA, # 5401119001), a blend of purified collagenases I and II, to prepare a single cell suspension of MV cells. Isolated cells were fixed using Flow Cytometry Fixation Buffer (R&D Systems, MN, USA, #FC004) and labeled in Flow Cytometry Permeabilization/Wash Buffer I (R&D Systems, MN, USA, #FC005) for 45 minutes (100,000 cells/100 μl Buffer I). Murine anti-sheep CD45-FITC or -APC (1:50; AbD Serotec, NC, USA, # MCA2220F, #MCA2220GA, #MCA896GA, LYNX Rapid APC Antibody Conjugation Kit, #LNK031APC), VE-cadherin-PE or -FITC (1:100; R&D Systems, MN, USA, # FAB9381P and AbD Serotec, NC, USA, # AHP628F), and α-smooth muscle actin

(αSMA)-APC or -PE (1:100; R&D Systems, MN, USA, # IC1420P and # IC1420A) were used. All antibodies were shown to cross-react with their ovine homologs.

Cell culture

Ovine mitral VEC clones and carotid artery endothelial cells (CAEC) were isolated[14] and grown on 1% gelatin-coated dishes in EBM-2 medium (Lonza Inc., GA, USA #CC-3156) supplemented with 10% heat-inactivated FBS, 1% glutamine-penicillin-streptomycin sulfate (Life Technologies, cat# 10378-016) and 2ng/ml basic fibroblast growth factor (Roche LifeScience, IN, USA, cat # 11123149001), henceforth referred to as EBM-B.

EndMT assay

Ovine mitral VEC and CAEC were plated on gelatin-coated plates at 10,000 cells/cm^2. After 24 hours, EBM-B was replaced with fresh EBM-B containing 1ng/ml human TGFβ1 (R&D Systems, MN, USA #100-B-001). Cells were harvested with Liberase (100μL/cm^2) 96 hours later, and used for flow cytometry, quantitative PCR or migration assays. For flow cytometry, cells were analyzed simultaneously for VE-cadherin, α-SMA and CD45 as described above.

Quantitative PCR (qPCR)

Ovine mitral VEC and CAEC were subjected to the EndMT assay in the presence or absence of 0.5μmol/L *N*-(9,10-dioxo-9,10-dihydro-phenanthren-2-yl)-2,2-dimethyl propionamide, a CD45-selective protein tyrosine phosphatase (PTPase) inhibitor (EMD Millipore Sigma, MA, USA# 540215) [21]. Total cellular RNA was extracted from mitral VEC clones (C5, D1, E5, E10 and E10-2) and CAEC (n=2) with an RNeasy Micro extraction kit (Qiagen, Valencia, CA, #74004). Reverse transcriptase reactions were performed using an iScript cDNA Synthesis Kit (Bio-Rad, CA, USA #170-8890). qPCR was performed using Kapa Sybr Fast ABI Prism 2x qPCR Master Mix (KAPA BioSystems, MA, USA # KK4604). Amplification was carried out in an ABI 7500 (Applied Biosystems, Foster City, CA). A standard curve for each gene was generated to determine amplification efficiency. RPS9 was used as housekeeping gene expression reference. Fold increases in gene expression were calculated according to 2 delta C_T method [22, 23], with each amplification reaction performed in triplicate.

Cellular migration assay

Mitral VEC clones (D1, E5, E10-2) or CAEC were treated ± TGFβ for 4 days to induce EndMT. The cells were treated for 30 minutes ± the CD45-selective PTPase inhibitor (1μmol/L)[21] prior to trypsinization. 20,000 cells (± PTPase inhibitor 1μmol/L) in 0.1% BSA/EBM-2 (Lonza) were placed in the upper chamber of 6.5mm Transwells containing fibronectin-coated (0.2 ug/cm2) polycarbonate membranes with 8.0μm pores. The lower chambers contained 0.1% BSA/EBM-2 media alone or EBM with serum and basic FGF as a chemoattractants. Cells were allowed to migrate for 6 hours at 37°C. Cells that migrated through the pores were fixed with methanol and stained with Eosin-Y, Azure A and Methylene Blue for visualization and quantification using Three Step Stain Set (VWR, PA,

USA #48218-567). In parallel, an aliquot of cells used for the migration assay were also analyzed for CD45 by flow cytometry to verify response to TGFβ1.

Statistics

Sample variances were analyzed by Fisher tests to determine equal or non-equal variances. A Fisher p-value > 0.05 was considered equal variance. In Table 1, equal variances were found for all comparisons. Two-tailed, two sample t-tests were performed. In Figures 4 and 5, fold changes are reported as mean ± standard deviation (SD). In Figure 4, qPCR data from 5 different mitral valve VEC clones were standardized as described Willems [24]. In Figures 4 and 5, data were analyzed by one-way ANOVA, Fisher Tests, and two-tailed two independent sample T-Tests. Statistical programs were from Excel and XLStat Pro. In Figure 6, linear regression analysis was performed and the R-squared value was calculated to see how well the regression line fit the data. $P < 0.05$ was considered significant.

RESULTS

CD45 expression in mitral valve endothelium post-MI

A total of 5 sheep underwent IMI and were euthanized 6 months after the procedure. All infarcted sheep developed MR, as determined by color-doppler echocardiography at the time of sacrifice. Sham (n= 5) and normal (n=3) were analyzed as well (Online Table I). Because of the known inflammatory state associated with MI, we assessed the presence of leukocytes in MV by staining for CD45, a receptor-like protein tyrosine phosphatase (PTPase) expressed in all leukocytes. Strong immunostaining for CD45 was seen on the endothelial and sub-endothelial layers on the atrial side of the IMI MVs as well as the interstitial regions (Fig A, D). CD45 expression was less evident in control MVs (Fig 1B) and was not detected in IMI MV stained with an isotype-matched control IgG (Fig 1C). For comparison, CD14, expressed on macrophages and, to a lesser extent, neutrophils, was detected in the interstitial region of IMI MVs but not along the endothelium (Fig 1E). CD45 was not detected in MVs from a mitral regurgitation (MR) only model, in which there was no MI, only a posterior leaflet retraction to produce MR (Fig 1F). Double immunofluorescent staining of IMI MVs showed CD45 co-localized with von Willebrand Factor, a glycoprotein expressed in endothelial cells[25] (Fig 1G-J). Results from these two immunostaining experiments indicated that mitral VECs might contribute to the CD45+ cell population in IMI MVs. CD45 was also partially co-localized with αSMA+ cells in IMI MV leaflets (Online Figure IA). Based on this, we hypothesized that some of the CD45+ cells could be endothelial cells undergoing EndMT or fibrocytes, which are myeloid fibroblasts that express αSMA and produce collagen[12, 26]. αSMA and increased collagen are both hallmarks of MV adaptation to IMR [5, 8].

Quantification of CD45-positive cells in MVs by triple-label flow cytometry

To pursue the endothelial-localized CD45 expression, we devised a method to gently release cells from MV leaflet tissue immediately after removal from sheep and quantify the relative proportions of endothelial, interstitial and hematopoietic cell populations. MV leaflet tissue was minced into small pieces and digested with a mix of type I and II collagenases for 30 minutes at 37 °C to generate a single cell suspension. Cells were permeabilized, and

simultaneously incubated with anti-VE-cadherin-PE (endothelial marker), anti-CD45-FITC (hematopoietic/fibrocyte marker) and anti-αSMA-APC (myofibroblast/fibrocyte marker). This allowed us to identify and quantify 8 distinct cell populations (Figure 2 and Table 1). The co-expression of CD45 in VE-cadherin-positive endothelial cells (Fig 2, top row, pink shaded quadrant) confirmed the CD45-positive endothelium detected in Figure 1. Furthermore, VE-cadherin+/CD45+/αSMA- and VE-cadherin+/CD45+/αSMA+ cells were significantly increased in IMI MVs compared to sham MVs (Table 1). VE-cadherin-/CD45+/αSMA+ cells, which we designated fibrocytes[27, 28], were also significantly increased in IMI MVs compared to sham MVs (Table 1). The flow cytometric analysis provided additional information on the cellular composition of the ovine mitral valve and how it changed after IMI. Cells with a quiescent valve interstitial cell (VIC) phenotype, VE-cadherin-/CD45-/αSMA-, were the most abundant in the MV but were not significantly different between IMI and sham MVs (Table 1). Activated VICs (VE-cadherin-/CD45-/αSMA+) were detected in both sham and IMI valves but also did not differ significantly by this method of analysis. Hematopoietic cells, defined as VE-cadherin-/CD45+/αSMA-, were present and not significantly changed. From Table 1, one can calculate that MV endothelial cells constituted 64% of the total CD45+ cells, hematopoietic cells 21% and fibrocytes 14% in this 6 month IMI model. This demonstrates that at 6 months post-IMI, the majority of the CD45+ cells in the MV are endothelial cells.

For comparison, the flow cytometry analysis was also performed on MVs from normal sheep (Online Table II). The normal MVs were comprised of primarily VE-cadherin+/CD45-/αSMA- endothelial cells (38%) and VE-cadherin-/CD45-/αSMA- cells (57%), which we designate quiescent VICs. There were very few CD45+ or α-SMA+ cells indicating a quiescent, non-inflammatory, non-fibrotic state.

TGFβ1 induces CD45 in mitral VEC, coincident with EndMT

The presence of CD45 and αSMA in VE-cadherin-positive cells in IMI MVs suggested that CD45 induction may coincide with EndMT processes [29]. Our previous work showed increased EndMT, also called EMT, in tethered MVs in an ovine model, and suggested EndMT as a possible contributor to growth of MV leaflets to minimize mitral regurgitation[5]. To assess the link between EndMT and CD45, mitral VEC clones (prepared by expansion from a single mitral VEC[14]) and CAECs (incapable of undergoing EndMT[14]) were tested for CD45 expression in response to TGFβ1. *In vitro* treatment of mitral VEC clone E10 with TGFβ1 led to strong induction of CD45 and αSMA, detected by flow cytometry (Fig 3A, B). Interestingly, 23–25% of the mitral VEC clone E10 cells showed a low level of CD45 expression prior to TGFβ treatment (Fig 3A). Non-treated and TGFβ1-treated CAECs did not express CD45 or αSMA (Fig 3C and D). Analysis of four additional mitral VEC clones treated with TGFβ1 showed that the percent CD45-positive cells ranged from 19–88% in these clones (Fig 3E). In TGFβ1 non-treated VEC clones, CD45-positive cells ranged from 3–40% (not shown). In total, seven mitral VEC clones were studied: CD45 was significantly increased after 4 day exposure to TGFβ1 ($P = 0.029$ by paired *t*-test). αSMA was also significantly increased in TGFβ1-treated mitral VEC clones, as expected ($P = 0.007$ by paired *t*-test) (not shown). To determine if other hematopoietic markers were increased in TGFβ1-treated mitral VEC, we analyzed expression of CD11b (expressed on monocytes,

neutrophils, natural killer cells, granulocytes and macrophages) and CD14 (expressed on macrophages, neutrophils and dendritic cells) by flow cytometry (Online Figure II). No expression was detected, while CD45 was increased as expected. These results demonstrate that purified mitral VECs specifically express CD45, and the levels are significantly increased by TGFβ1.

CD45 PTPase inhibitor blocks expression of EndMT and fibrosis markers

To verify the increased CD45 detected by flow cytometry, we analyzed CD45 mRNA in TGFβ1-treated mitral VEC and CAEC by qPCR (Fig 4A, B). In parallel, VE-cadherin and αSMA were measured to assess EndMT. Data compiled from five different mitral VEC clones showed significant increases in CD45 (p=0.0001) and αSMA mRNA (p=0.0131) (Fig 4A). No changes in CD45, VE-cadherin or αSMA mRNA levels were seen in TGFβ1-treated CAEC (Fig 4B). Well-established EndMT markers Slug and MMP2[30, 31], and NFATc1, which is negatively correlated with EndMT[32], were modulated as expected in TGFβ1-treated mitral VEC, consistent with our previous study[15]. Collagen 1 and collagen 3 mRNA transcripts as well as TGFβ1, TGFβ2 and TGFβ3 were also increased in TGFβ1-treated mitral VEC clones (Fig 4C). Inclusion of a CD45-selective protein tyrosine phosphatase (PTPase) (0.5 μM) during the 4 day TGFβ1 treatment significantly reduced αSMA, Slug, MMP-2, collagen 1, collagen 3, TGFβ1, TGFβ2 and TGFβ3 mRNA levels and restored NFATc1 mRNA (Fig 4C). P-values for Figure 4C are provided in Online Table III. In contrast, no changes in these markers were seen in TGFβ1-treated CAEC, in the presence or absence of the CD45 PTPase inhibitor (Fig 4D). These results suggest that CD45 plays a functional role in EndMT and transition of mitral VEC to a fibrotic phenotype.

CD45 PTPase inhibition reduced EndMT-associated migration

Increased migration is a hallmark of endothelial cells undergoing EndMT[33, 34]. Therefore, we examined the requirement for ongoing CD45 phosphatase activity in migration of endothelial cells induced to undergo EndMT (Fig 5). Mitral VEC and CAEC were treated without (gray bars) or with TGFβ1 for 4 days (black bars). Cells were then treated with or without CD45 PTPase inhibitor (1.0 μM) for 30 min, removed from culture dishes with trypsin, and resuspended in endothelial basal media (EBM) without serum and growth factors, ± 1.0 μM CD45 PTPase inhibitor. The cells were then assayed for migration towards EBM or EBM with serum and basic fibroblast growth factor (bFGF) added as chemoattractants[35]. TGFβ-treated mitral VEC clones (n=3) showed significantly increased migration towards serum and bFGF (p=0.0145), which was significantly inhibited by the CD45 PTPase inhibitor (p=0.0100) (Fig 5A). Both control and TGFβ1-treated CAEC showed modest but significantly increased migration towards serum and bFGF in the 6 hour migration assay (p=0.0249; p=0.0141, respectively), but showed no increase in migration after TGFβ treatment and no response to the CD45 PTPase inhibitor (Fig 5B). An aliquot of mitral VEC and CAEC used for the migration assay was assayed for CD45 by flow cytometry to verify CD45 was expressed in the mitral VEC and not in the CAEC (data not shown). These results further suggest that CD45 plays a functional role in EndMT.

Increase in CD45+ cells at 6 months post-IMI correlates with MV fibrosis and MR severity

To determine if CD45+ MV cells associate with detrimental impacts, MVs were analyzed histologically and functionally. To assess collagen accumulation, which would stiffen the MV leaflets and impair their ability to form an effective seal to prevent MR, MV sections from sham (n=5) and IMI-6 month (n=5) sheep were analyzed by Masson Trichrome stain (Fig 6A). Quantification of the percent positive area showed significantly increased collagen in the IMI-6 MVs (Fig 6B), which correlated with increased CD45+ cells detected by immunohistochemistry (Fig 6C). The excessive and disordered collagen detected by Masson Trichrome in the IMI-6 MV is a hallmark of fibrosis.

Total CD45+ cells in individual IMI-6 month MVs, measured by flow cytometry, showed a positive correlation with infarct surface area relative to the total left ventricular endocardial surface area (ESA) (R^2 = 0.83, p= 0.02) (Fig 6D). The vena contracta width (VCW) indicating mitral regurgitation severity was measured in all sheep, sham (×) and IMI-6 month (▲), and plotted against CD45+ cells that increased 6 months after IMI (Table 1). These CD45+ cells (VE-cadherin+/CD45+/αSMA+, VE-cadherin+/CD45+/α-SMA-, and VE-cadherin-/CD45+/αSMA+) showed a strong correlation (R^2=0.72, p= 0.002) with the VCW (Fig 6E). Global LV remodeling was assessed by measuring the total LV ESA ratio between immediately post-MI (T1) and 6 months (T2) by 3-dimensional echocardiography[16–19] This remodeling ratio showed a strong positive correlation with the MV CD45+ cells (R^2=0.79, p<0.001).This suggests that not only the infarct size but left ventricular remodeling exerts an effect on the MV and in turn the number of CD45-expressing cells in the leaflets. The cell-modifying stimulus could be attributed to prolong cytokine release occurring after LV damage and failure, as has been described[36]. CD45+ cells showed a negative correlation with ejection fraction (R^2=0.71, p= 0.002) (Fig 6G).

DISCUSSION

In this study we identify an unanticipated expression of CD45 in mitral VEC both *in vivo* post-MI and *in vitro* in response to TGFβ1. At 6 months post-MI, CD45+ endothelial cells were the most abundant CD45+ cell population in the MV. This was determined by flow cytometry, an objective and quantitative method carried out on single cell preparations from collagenase-digested anterior and posterior MV leaflets. A large fraction of the CD45+ endothelial cells co-expressed αSMA, which suggested the cells were undergoing EndMT. CD45+/αSMA+ cells were also detected and significantly increased in 6 months-IMI MVs. The increases in CD45+ cells correlated with MV fibrosis, MR severity and infarct size. *In vitro*, ovine mitral VECs expressed a low level of endogenous CD45, which was increased significantly by TGFβ1, with concomitant, significant increases in αSMA, additional EndMT markers, and collagen 1, collagen 3, TGFβ1, TGFβ1 and TGFβ3; such cytokine self-amplification has been described previously [36]. A CD45-selective PTPase inhibitor modulated expression of all of these markers. The CD45 PTPase inhibitor also blocked EndMT-associated increased migration of mitral VEC. These assays were conducted on several different mitral VEC clones, indicating robust findings. Combined, these results suggest a functional role for CD45 in EndMT and induction of a collagen-producing, TGFβ-producing cellular phenotype that could portend fibrosis. Consistent with this idea, increased

collagen accumulation, indicative of fibrosis, was coincident with increased CD45+ cells in the IMI-6 MVs.

CD45 is best known as a transmembrane glycoprotein expressed on all differentiated hematopoietic cells, except erythrocytes and platelets. As such, it is often used as a marker for cells of hematopoietic origin, and it is commonly used to isolate leukocytes. CD45 regulates a variety of cellular processes including cell migration, proliferation, and differentiation [373839]. In light of its known roles in cellular motility and migration of hematopoietic cells, it is interesting that CD45 also appears to play a role in migration of mitral VEC that have become activated to undergo EndMT. Through its intrinsic phosphatase activity CD45 can either dampen or activate signaling pathways by dephosphorylating Src kinase family members, in particular Lck in T cells and Lyn in B cells[38]. CD45 can also affect integrin-mediated adhesion in T cells and macrophages by down regulating the activity of Src family kinases Lyn and Hck, limiting their participation in the formation of stable focal adhesions[38]. Bone marrow-derived mononuclear cells from CD45 knockout mice show increased adhesion and decreased migration[40], activities that would counteract EndMT processes. Further, the CD45 knockout cells showed increased Src and phosphorylated Erk[40]. An analysis of Src family kinases as potential targets of VEC CD45 would be a topic of future studies.

CD45 is not normally expressed on endothelium or endothelial cells. An exception is during embryonic development when specific sites within the yolk sac, the placenta and the dorsal aorta become “hemogenic” for a narrow window of time. CD45+/VE-cadherin+ cells bud from the hemogenic endothelium to give rise to hematopoietic stem cells[41, 42]. Purified cultures of human endothelial cells are typically devoid of CD45+ cells[43], although we detected a limited window of hemogenic activity in human umbilical cord blood CD133-selected endothelial colony forming cells[44]. No CD45+ adult endothelium has been described so far. Therefore, our discovery of CD45+ endothelial cells in MVs at 6 months post-IMI and in cultured mitral VECs is novel. Further, we show CD45 is not expressed in arterial endothelial cells treated with or without TGFβ, indicating selectivity. We also showed that hematopoietic markers, such as CD14 and CD11b, were not increased in mitral VEC by TGFβ1, nor was CD14 detected along the endothelium in mitral valves from IMI sheep at 6 months.

We postulate that endothelial CD45 is important in the MV adaptive response post-MI and further, the response encompasses both pro- and maladaptive processes. We recently reported a constellation of cellular changes in MV leaflets in an ovine model of tethering plus MI, which included significantly increased CD45+ cells at 2 months, as well as significantly increased EndMT[8]. In that study, we had not yet developed the triple-label flow cytometric method to quantify the 8 distinct cell populations in MV, and therefore do not know the distribution of CD45+ cells among endothelial cells, hematopoietic cells and fibrocytes. In the current study, we show that in the 6 months IMI model, MV endothelial cells constituted 64% of the total CD45+ cells, hematopoietic cells 21% and fibrocytes 14%. We postulate that increased endothelial CD45, with its intrinsic phosphatase activity, may decrease adhesion and/or increase migration of mitral VECs, as CD45 has been implicated in these cellular activities[20, 39, 41]. Indeed, increased migration is a hallmark of cells

undergoing EndMT[29], which we speculate is an important process used to replenish mitral VICs and increase MV leaflet area[5, 35]. The EndMT could be pro-adaptive if it proceeded in a regulated manner to produce VICs; on the other hand, if EndMT is uncontrolled, it may result in maladaptive valve growth. EndMT has recently been implicated other maladaptive settings, such as atherosclerotic lesions and plaque instability[45].

Approximately 15% of the $CD45^+$ cells in the IMI-6 months MVs may be fibrocytes, also known as myeloid fibroblasts[26], based on the co-expression of CD45 and αSMA and lack of VE-cadherin. CD45 suggests a hematopoietic origin of fibrocytes/myeloid fibroblasts and αSMA indicates myofibroblastic functionality[12]. Despite their relatively low number in IMI MVs, the fibrocytes may be an important factor in the maladaptive MV response to MI, as these cells can release inflammatory and fibrogenic growth factors, including TNFα, IL6, IL8, TGFβ1–3, collagen I and III, and fibronectin[46] and importantly have been shown to contribute to cardiac fibrosis[26], including fibrosis post-MI[47, 48]. The possibility that MV CD45+ cells after MI contribute to a self-reinforcing fibrotic cycle merits exploration for potential therapeutic directions; targets could include both fibrocytes and CD45+ VEC undergoing EndMT. In myxomatous MVs, fibrocytes are increased under pro-fibrotic conditions[49], supporting their role in collagen deposition in the valves. Hajdu and colleagues identified a fibrocyte-like population in normal murine mitral valve leaflets that are spindle-shaped, CD45-positive and bone marrow-derived. They further characterized the cells as vimentin-positive but endothelial and leukocyte marker negative[50]. They concluded that bone marrow-derived cells contribute to the VIC population under normal homeostatic conditions. The increased CD45+/αSMA+ cell population in the ovine IMI MVs may be related to this phenomenon, but would likely reflect an enhancement or exaggeration of the steady state influx of bone marrow cells into the MV. An alternative hypothesis, given the capability of mitral VEC to express collagen I, collagen 3 and TGFβ1, TGFβ2 and TGFβ3 (Figure 4C), is that some VE-cadherin+/CD45+/αSMA+ endothelial cells might downregulate VE-cadherin and become resident CD45+/αSMA+ fibrocytes. The possibility that mitral VEC may contribute directly to the fibrocyte population merits investigation.

In summary, here we provide a relative quantification of multiple cell types in MVs at 6 months post-MI using an objective and unbiased method, similar to a recent report on murine cardiac cellular composition[51]. The identification of a CD45+ endothelial population suggests upregulated endothelial CD45 may play a role in adaptation of MV cells post-MI. Given the plasticity of mitral VECs [14], CD45 may be an indicator of an adaptive phenotype. Finally, these results identify a functional role for CD45 protein tyrosine phosphatase in EndMT, an entirely novel finding that warrants further investigation. That CD45+ cells were found associated with adverse outcomes including leaflet fibrosis, MR severity, LV remodeling and reduced ejection fraction provides a strong rationale for pursuit of such studies.

Supplementary Material

Refer to Web version on PubMed Central for supplementary material.

Acknowledgments

SOURCES OF FUNDING

Research reported in this manuscript was supported by *the NHLBI* of the National Institutes of Health under award number R01HL109506-01A1, to E. A., J. B., and R.A.L. The content is solely the responsibility of the authors and does not necessarily represent the official views of the National Institutes of Health. The study was also supported initially by the Fondation Leducq Transatlantic Network (J.B, E.A. and R.A.L.)”

Nonstandard Abbreviations and Acronyms

MV	mitral valve
IMI	inferior myocardial infarction
α-SMA	α-smooth muscle actin
EndMT	endothelial-to-mesenchymal transition
VEC	valve endothelial cell
VIC	valve interstitial cell
MR	mitral regurgitation
CAEC	carotid artery endothelial cell
FBS	fetal bovine serum
TGFβ	transforming growth factor-β
PTPase	protein tyrosine phosphatase
ESA	endocardial surface area
VCW	vena contracta width

REFERENCES

1. Levine RA, Schwammenthal E. Ischemic mitral regurgitation on the threshold of a solution: From paradoxes to unifying concepts. Circulation. 2005; 112:745–758. [PubMed: 16061756]
2. Walker GA, Masters KS, Shah DN, Anseth KS, Leinwand LA. Valvular myofibroblast activation by transforming growth factor-beta: Implications for pathological extracellular matrix remodeling in heart valve disease. Circ Res. 2004; 95:253–260. [PubMed: 15217906]
3. Grande-Allen KJ, Barber JE, Klatka KM, Houghtaling PL, Vesely I, Moravec CS, McCarthy PM. Mitral valve stiffening in end-stage heart failure: Evidence of an organic contribution to functional mitral regurgitation. J Thorac Cardiovasc Surg. 2005; 130:783–790. [PubMed: 16153929]
4. Grande-Allen KJ, Borowski AG, Troughton RW, Houghtaling PL, Dipaola NR, Moravec CS, Vesely I, Griffin BP. Apparently normal mitral valves in patients with heart failure demonstrate biochemical and structural derangements: An extracellular matrix and echocardiographic study. Journal of the American College of Cardiology. 2005; 45:54–61. [PubMed: 15629373]
5. Dal-Bianco JP, Aikawa E, Bischoff J, Guerrero JL, Handschumacher MD, Sullivan S, Johnson B, Titus JS, Iwamoto Y, Wylie-Sears J, Levine RA, Carpentier A. Active adaptation of the tethered mitral valve: Insights into a compensatory mechanism for functional mitral regurgitation. Circulation. 2009; 120:334–342. [PubMed: 19597052]

6. Kakio T, Matsumori A, Ono K, Ito H, Matsushima K, Sasayama S. Roles and relationship of macrophages and monocyte chemotactic and activating factor/monocyte chemoattractant protein-1 in the ischemic and reperfused rat heart. Laboratory investigation; a journal of technical methods and pathology. 2000; 80:1127–1136. [PubMed: 10908159]
7. Brands M, Roelants J, de Krijger R, Bogers A, Reuser A, van der Ploeg A, Helbing W. Macrophage involvement in mitral valve pathology in mucopolysaccharidosis type vi (maroteaux-lamy syndrome). Am J Med Genet A. 2013; 161A:2550–2553. [PubMed: 23949968]
8. Dal-Bianco JP, Aikawa E, Bischoff J, Guerrero JL, Hjortnaes J, Beaudoin J, Szymanski C, Bartko PE, Seybolt MM, Handschumacher MD, Sullivan S, Garcia ML, Mauskapf A, Titus JS, Wylie-Sears J, Irvin WS, Chaput M, Messas E, Hagege AA, Carpentier A, Levine RA. Myocardial infarction alters adaptation of the tethered mitral valve. J Am Coll Cardiol. 2016; 67:275–287. [PubMed: 26796392]
9. Molin DG, Bartram U, Van der Heiden K, Van Iperen L, Speer CP, Hierck BP, Poelmann RE, Gittenberger-de-Groot AC. Expression patterns of tgfbeta1-3 associate with myocardialisation of the outflow tract and the development of the epicardium and the fibrous heart skeleton. Dev Dyn. 2003; 227:431–444. [PubMed: 12815630]
10. Akhurst RJ, Lehnert SA, Faissner A, Duffie E. Tgf beta in murine morphogenetic processes: The early embryo and cardiogenesis. Development. 1990; 108:645–656. [PubMed: 1696875]
11. Huk DJ, Austin BF, Horne TE, Hinton RB, Ray WC, Heistad DD, Lincoln J. Valve endothelial cell-derived tgfbeta1 signaling promotes nuclear localization of sox9 in interstitial cells associated with attenuated calcification. Arteriosclerosis, thrombosis, and vascular biology. 2016; 36:328–338.
12. Duffield JS, Lupher M, Thannickal VJ, Wynn TA. Host responses in tissue repair and fibrosis. Annu Rev Pathol. 2013; 8:241–276. [PubMed: 23092186]
13. Strieter RM, Keeley EC, Hughes MA, Burdick MD, Mehrad B. The role of circulating mesenchymal progenitor cells (fibrocytes) in the pathogenesis of pulmonary fibrosis. J Leukoc Biol. 2009; 86:1111–1118. [PubMed: 19581373]
14. Wylie-Sears J, Aikawa E, Levine RA, Yang JH, Bischoff J. Mitral valve endothelial cells with osteogenic differentiation potential. Arterioscler Thromb Vasc Biol. 2011; 31:598–607. [PubMed: 21164078]
15. Wylie-Sears J, Levine RA, Bischoff J. Losartan inhibits endothelial-to-mesenchymal transformation in mitral valve endothelial cells by blocking transforming growth factor-beta-induced phosphorylation of erk. Biochem Biophys Res Commun. 2014; 446:870–875. [PubMed: 24632204]
16. Handschumacher MD, Lethor JP, Siu SC, Mele D, Rivera JM, Picard MH, Weyman AE, Levine RA. A new integrated system for three-dimensional echocardiographic reconstruction: Development and validation for ventricular volume with application in human subjects. J Am Coll Cardiol. 1993; 21:743–753. [PubMed: 8436757]
17. Jiang L, Morrissey R, Handschumacher MD, Vazquez de Prada JA, He J, Picard MH, Weyman AE, Levine RA. Quantitative three-dimensional reconstruction of left ventricular volume with complete borders detected by acoustic quantification underestimates volume. Am Heart J. 1996; 131:553–559. [PubMed: 8604637]
18. Picard MH, Wilkins GT, Ray PA, Weyman AE. Natural history of left ventricular size and function after acute myocardial infarction. Assessment and prediction by echocardiographic endocardial surface mapping. Circulation. 1990; 82:484–494. [PubMed: 2372895]
19. Picard MH, Wilkins GT, Ray PA, Weyman AE. Progressive changes in ventricular structure and function during the year after acute myocardial infarction. Am Heart J. 1992; 124:24–31. [PubMed: 1535474]
20. Aikawa E, Nahrendorf M, Sosnovik D, Lok VM, Jaffer FA, Aikawa M, Weissleder R. Multimodality molecular imaging identifies proteolytic and osteogenic activities in early aortic valve disease. Circulation. 2007; 115:377–386. [PubMed: 17224478]
21. Panchal RG, Ulrich RL, Bradfute SB, Lane D, Ruthel G, Kenny TA, Iversen PL, Anderson AO, Gussio R, Raschke WC, Bavari S. Reduced expression of cd45 protein-tyrosine phosphatase provides protection against anthrax pathogenesis. The Journal of biological chemistry. 2009; 284:12874–12885. [PubMed: 19269962]

22. Pfaffl MW. A new mathematical model for relative quantification in real-time rt-pcr. Nucleic Acids Res. 2001; 29:e45. [PubMed: 11328886]
23. Schmittgen TD, Livak KJ. Analyzing real-time pcr data by the comparative c(t) method. Nat Protoc. 2008; 3:1101–1108. [PubMed: 18546601]
24. Willems E, Leyns L, Vandesompele J. Standardization of real-time pcr gene expression data from independent biological replicates. Anal Biochem. 2008; 379:127–129. [PubMed: 18485881]
25. Yamamoto K, de Waard V, Fearns C, Loskutoff DJ. Tissue distribution and regulation of murine von willebrand factor gene expression in vivo. Blood. 1998; 92:2791–2801. [PubMed: 9763564]
26. Cieslik KA, Trial J, Crawford JR, Taffet GE, Entman ML. Adverse fibrosis in the aging heart depends on signaling between myeloid and mesenchymal cells; role of inflammatory fibroblasts. J Mol Cell Cardiol. 2014; 70:56–63. [PubMed: 24184998]
27. Herzog EL, Bucala R. Fibrocytes in health and disease. Exp Hematol. 2010; 38:548–556. [PubMed: 20303382]
28. Keeley EC, Mehrad B, Strieter RM. Fibrocytes: Bringing new insights into mechanisms of inflammation and fibrosis. The international journal of biochemistry & cell biology. 2010; 42:535–542. [PubMed: 19850147]
29. Kovacic JC, Mercader N, Torres M, Boehm M, Fuster V. Epithelial-to-mesenchymal and endothelial-to-mesenchymal transition: From cardiovascular development to disease. Circulation. 2012; 125:1795–1808. [PubMed: 22492947]
30. Lincoln J, Yutzey KE. Molecular and developmental mechanisms of congenital heart valve disease. Birth Defects Res A Clin Mol Teratol. 2011; 91:526–534. [PubMed: 21538813]
31. Tao G, Kotick JD, Lincoln J. Heart valve development, maintenance, and disease: The role of endothelial cells. Curr Top Dev Biol. 2012; 100:203–232. [PubMed: 22449845]
32. Wu B, Wang Y, Lui W, Langworthy M, Tompkins KL, Hatzopoulos AK, Baldwin HS, Zhou B. Nfatc1 coordinates valve endocardial cell lineage development required for heart valve formation. Circulation research. 2011; 109:183–192. [PubMed: 21597012]
33. Person AD, Klewer SE, Runyan RB. Cell biology of cardiac cushion development. International Review of Cytology. 2005; 243:287–335. [PubMed: 15797462]
34. von Gise A, Pu WT. Endocardial and epicardial epithelial to mesenchymal transitions in heart development and disease. Circulation research. 2012; 110:1628–1645. [PubMed: 22679138]
35. Paranya G, Vineberg S, Dvorin E, Kaushal S, Roth SJ, Rabkin E, Schoen FJ, Bischoff J. Aortic valve endothelial cells undergo transforming growth factor-beta-mediated and non-transforming growth factor-beta-mediated transdifferentiation in vitro. American Journal of Pathology. 2001; 159:1335–1343. [PubMed: 11583961]
36. Nian M, Lee P, Khaper N, Liu P. Inflammatory cytokines and postmyocardial infarction remodeling. Circulation research. 2004; 94:1543–1553. [PubMed: 15217919]
37. Shivtiel S, Kollet O, Lapid K, Schajnovitz A, Goichberg P, Kalinkovich A, Shezen E, Tesio M, Netzer N, Petit I, Sharir A, Lapidot T. Cd45 regulates retention, motility, and numbers of hematopoietic progenitors, and affects osteoclast remodeling of metaphyseal trabecules. J Exp Med. 2008; 205:2381–2395. [PubMed: 18779349]
38. Saunders AE, Johnson P. Modulation of immune cell signalling by the leukocyte common tyrosine phosphatase, cd45. Cell Signal. 2010; 22:339–348. [PubMed: 19861160]
39. Lai JC, Wlodarska M, Liu DJ, Abraham N, Johnson P. Cd45 regulates migration, proliferation, and progression of double negative 1 thymocytes. J Immunol. 2010; 185:2059–2070. [PubMed: 20624943]
40. Shivtiel S, Kollet O, Lapid K, Schajnovitz A, Goichberg P, Kalinkovich A, Shezen E, Tesio M, Netzer N, Petit I, Sharir A, Lapidot T. Cd45 regulates retention, motility, and numbers of hematopoietic progenitors, and affects osteoclast remodeling of metaphyseal trabecules. J Exp Med. 2008; 205:2381–2395. [PubMed: 18779349]
41. Zape JP, Zovein AC. Hemogenic endothelium: Origins, regulation, and implications for vascular biology. Semin Cell Dev Biol. 2011; 22:1036–1047. [PubMed: 22001113]
42. Oberlin E, El Hafny B, Petit-Cocault L, Souyri M. Definitive human and mouse hematopoiesis originates from the embryonic endothelium: A new class of hscs based on ve-cadherin expression. Int J Dev Biol. 2010; 54:1165–1173. [PubMed: 20711993]

43. Yoder MC, Mead LE, Prater D, Krier TR, Mroueh KN, Li F, Krasich R, Temm CJ, Prchal JT, Ingram DA. Redefining endothelial progenitor cells via clonal analysis and hematopoietic stem/progenitor cell principals. Blood. 2007; 109:1801–1809. [PubMed: 17053059]
44. Wu X, Lensch MW, Wylie-Sears J, Daley GQ, Bischoff J. Hemogenic endothelial progenitor cells isolated from human umbilical cord blood. Stem Cells. 2007; 25:2770–2776. [PubMed: 17641248]
45. Evrard SM, Lecce L, Michelis KC, Nomura-Kitabayashi A, Pandey G, Purushothaman KR, d'Escamard V, Li JR, Hadri L, Fujitani K, Moreno PR, Benard L, Rimmele P, Cohain A, Mecham B, Randolph GJ, Nabel EG, Hajjar R, Fuster V, Boehm M, Kovacic JC. Endothelial to mesenchymal transition is common in atherosclerotic lesions and is associated with plaque instability. Nat Commun. 2016; 7:11853. [PubMed: 27340017]
46. Pilling D, Fan T, Huang D, Kaul B, Gomer RH. Identification of markers that distinguish monocyte-derived fibrocytes from monocytes, macrophages, and fibroblasts. PLoS One. 2009; 4:e7475. [PubMed: 19834619]
47. Nian M, Lee P, Khaper N, Liu P. Inflammatory cytokines and postmyocardial infarction remodeling. Circ Res. 2004; 94:1543–1553. [PubMed: 15217919]
48. Bujak M, Frangogiannis NG. The role of tgf-beta signaling in myocardial infarction and cardiac remodeling. Cardiovasc Res. 2007; 74:184–195. [PubMed: 17109837]
49. Barth PJ, Koster H, Moosdorf R. Cd34+ fibrocytes in normal mitral valves and myxomatous mitral valve degeneration. Pathol Res Pract. 2005; 201:301–304. [PubMed: 15991836]
50. Hajdu Z, Romeo SJ, Fleming PA, Markwald RR, Visconti RP, Drake CJ. Recruitment of bone marrow-derived valve interstitial cells is a normal homeostatic process. J Mol Cell Cardiol. 2011; 51:955–965. [PubMed: 21871458]
51. Pinto AR, Ilinykh A, Ivey MJ, Kuwabara JT, D'Antoni ML, Debuque R, Chandran A, Wang L, Arora K, Rosenthal NA, Tallquist MD. Revisiting cardiac cellular composition. Circulation research. 2016; 118:400–409. [PubMed: 26635390]

Novelty and Significance

What Is Known?

- After inferior myocardial infarction (IMI), progressive mitral valve (MV) regurgitation develops that increases heart failure and mortality, and is difficult to repair.
- While MV leaflet tethering causes compensatory valve enlargement, associated with endothelial-to-mesenchymal transition (EndMT), MI combined with leaflet tethering induces counterproductive MV fibrosis that impairs leaflet closure and increases regurgitation.
- This post-MI fibrotic process is associated with excessive EndMT and CD45-positive cells in the MV, and TGFβ protein in MV cells.

What New Information Does This Article Contribute?

- Unexpectedly, the CD45+ cells in the ovine six-month post-MI MV co-express endothelial markers, many localize within the endothelium or sub-endothelium, and express markers consistent with EndMT. The proportion of CD45+ cells in these valves correlates with valve fibrosis (collagen content) and MR severity as well as infarct size and left ventricular remodeling (dilation).
- In vitro, TGFβ specifically induces ovine MV endothelial cells to undergo EndMT, migrate, and express CD45, collagen and intrinsic TGFβ, all blocked by a CD45-selective protein tyrosine phosphatase inhibitor.

MI is accompanied by adaptive enlargement of the tethered MV combined with maladaptive fibrosis that limits leaflet expansion and promotes mitral regurgitation through as yet unknown cellular processes. MV EndMT appears to play a role in the initial enlargement and new findings here indicate it may be a substrate for fibrosis. There are substantially increased cells expressing CD45, a protein tyrosine phosphatase, in the MV at 6 months post-inferior MI. The majority of the MV CD45+ cells have an intrinsic endothelial phenotype with indicators of ongoing EndMT. The increase in CD45+ cells is correlated with MV collagen deposition, infarct size and MR severity in the ovine inferior MI model. In vitro, TGFβ, which is released in the post-MI inflammatory state, induced CD45+ expression in MV endothelial cells, coincident with increased cell migration, a hallmark of EndMT, and expression of EndMT markers and the fibrosis markers collagens 1 and 3 and endogenous TGFβ1–3. A CD45-selective phosphatase inhibitor blocked the increased migration and expression of EndMT and fibrosis markers, which suggests a functional role for CD45 in EndMT and the production of fibrotic cells. These findings suggest new avenues for understanding mechanisms driving MV regurgitation and point to new therapeutic opportunities.

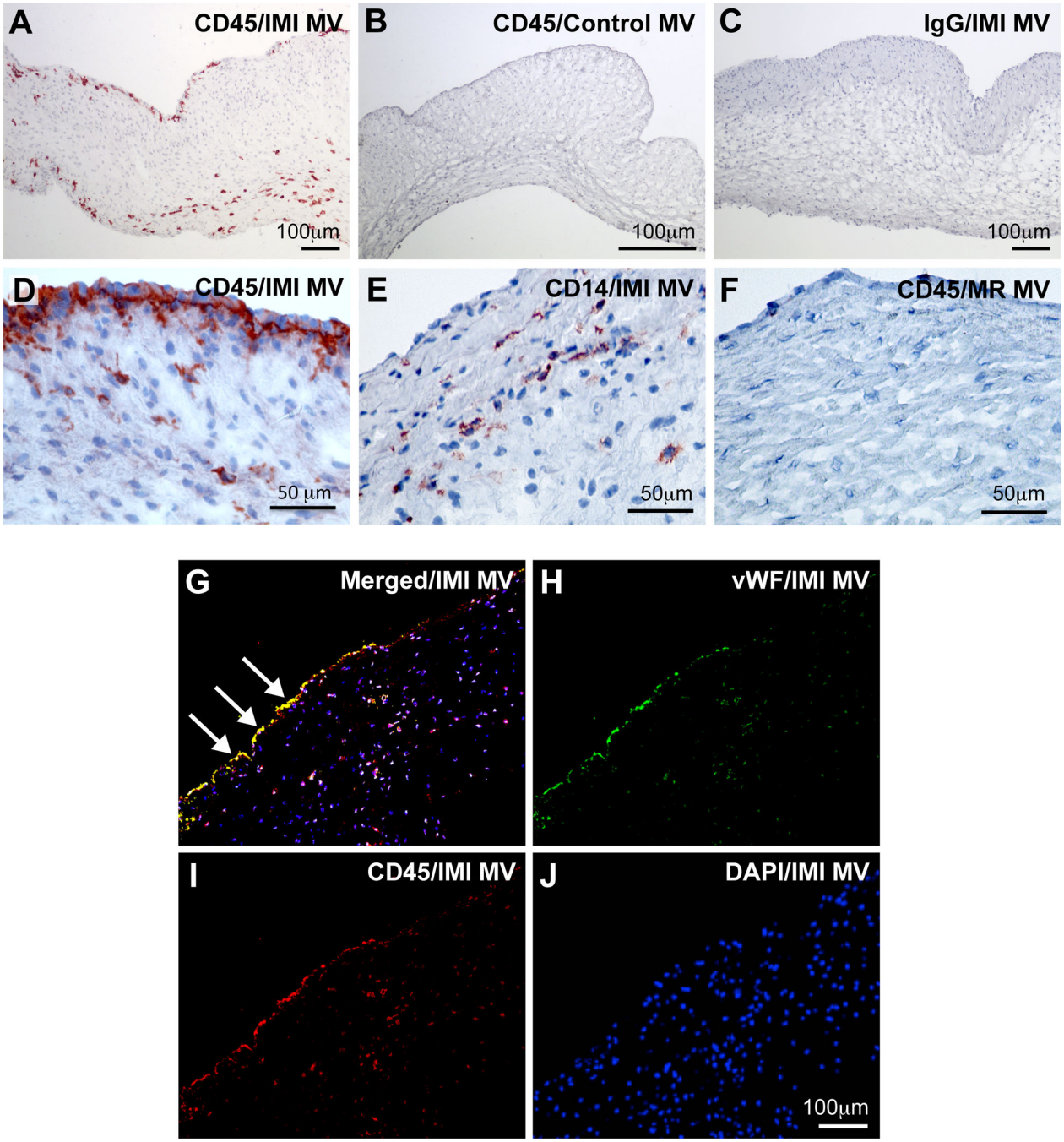

Figure 1. CD45 detected in the mitral valve endothelium post-MI

(A-F) Immunohistochemical staining of MV leaflets: anti-CD45 staining (A, B, D, F), control IgG staining (C). anti-CD14 staining (E). Ovine MV leaflets from animals 6 months after IMI (A, C, D, E), control animals (B) and mitral regurgitation (MR) only animals (F). (G-J) Immunofluorescence staining of IMI 6-months MV leaflets. Panel G shows double-staining with anti-CD45 and anti-von Willebrand factor (vWF), an endothelial marker. Arrows mark endothelial cells co-expressing CD45 and vWF. Panel H shows single staining

with anti-vWF. Panel I shows single staining with anti-CD45 and Panel J shows DAPI staining only.

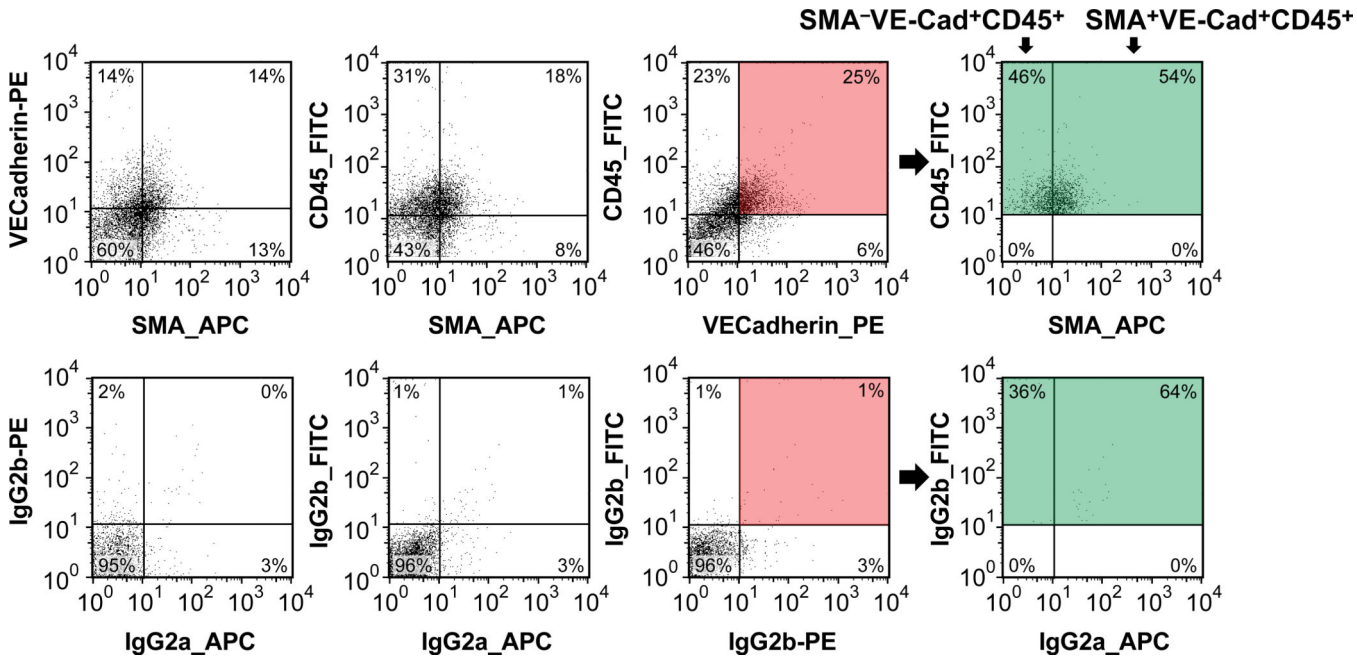

Figure 2. CD45/VE-Cadherin/αSMA analysis of MV cells 6 months after inferior MI (IMI)

A representative flow cytometric analysis is shown. Top panels show the labeling for VE-cadherin, αSMA and CD45. VE-Cadherin-positive/CD45-positive cells (pink-shaded box) were analyzed in the APC-channel (green-shaded box) for αSMA-positive cells. This shows the distribution of VE-cadherin-positive/CD45-positive cells into αSMA-negative and αSMA-positive subpopulations. Bottom row shows cells labeled with isotype-matched IgGs to establish background staining. A summary of the complete flow cytometric analysis is shown in Table 1.

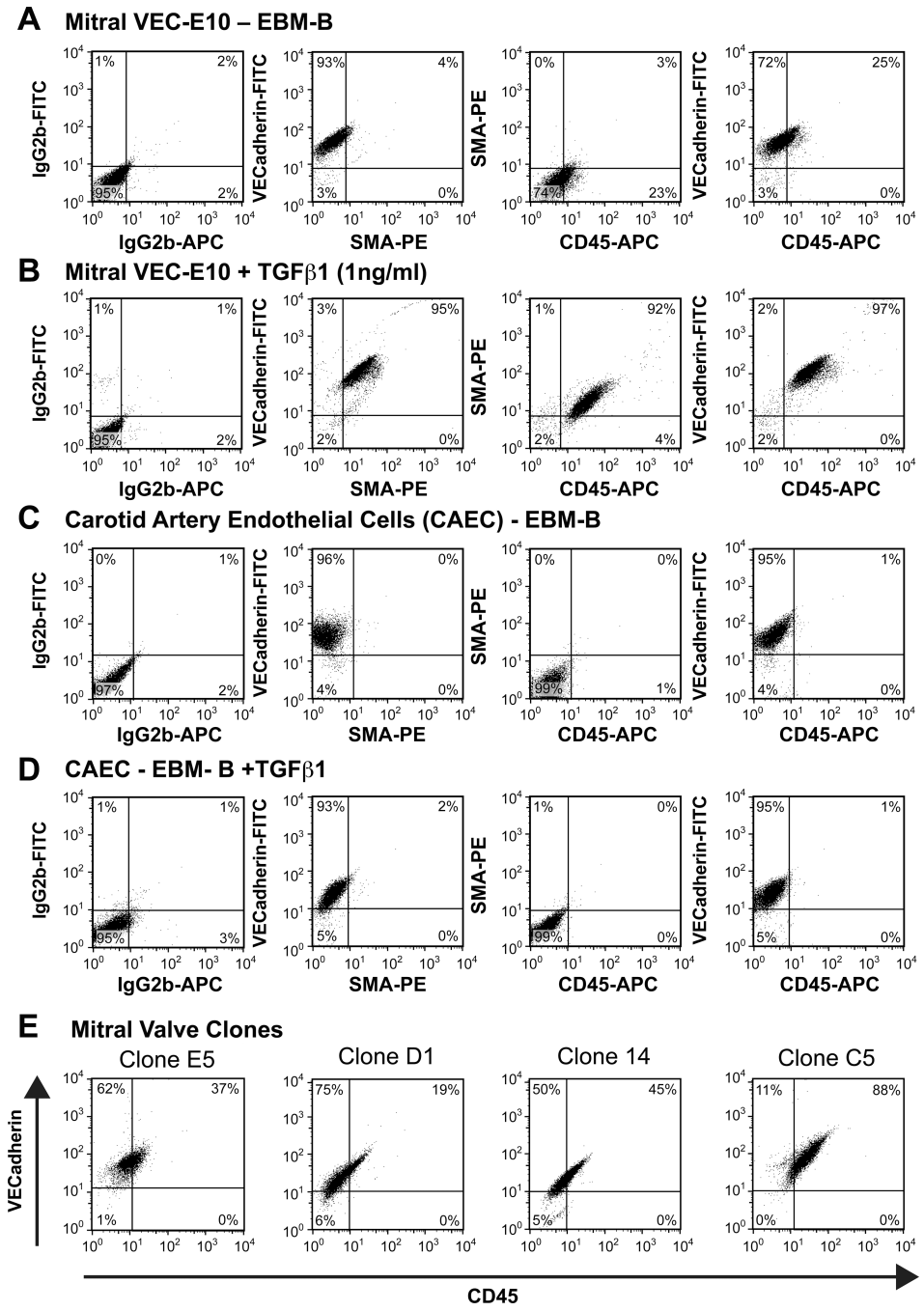

Figure 3. Flow cytometry of mitral VEC clones and non-valvular CAEC

Mitral VEC clone E10 (A, B) and CAECs (C, D) treated with EBM-B (A, C) or EBM-B + 1ng/mL TGFβ1 (B, D) for 4 days to induce EndMT. E) Four additional mitral VEC clones treated with EBM-B + 1ng/mL TGFβ1 for 4 days. Each mitral VEC clone, E5, D1, I4 and C5, was analyzed for VE-cadherin and CD45 to show the range of CD45 expression among mitral VEC clones.

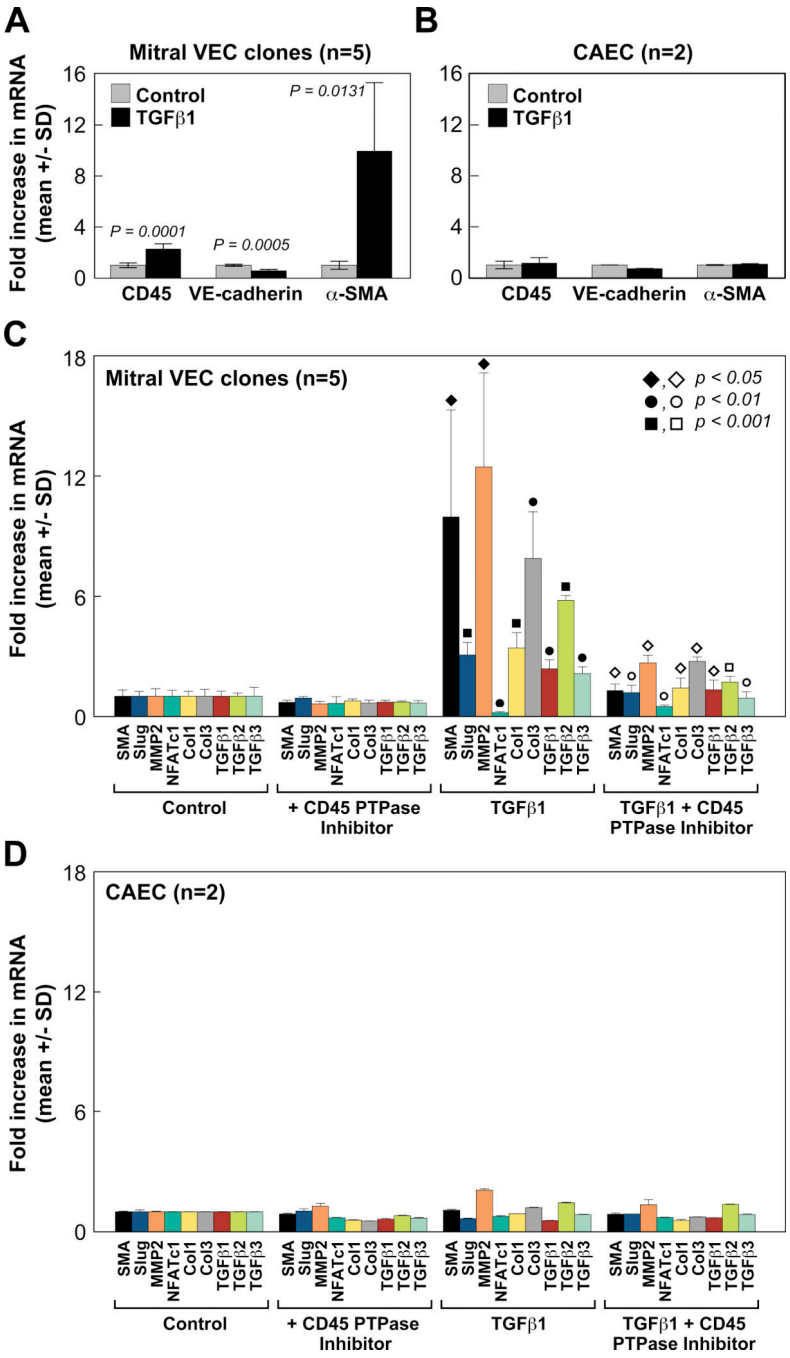

Figure 4. Increased EndMT and fibrosis markers blocked by CD45 PTPase inhibitor

(A, B) CD45, VE-cadherin and αSMA mRNA levels in mitral VEC clones and CAEC measured by qPCR. Cells were treated for 4 days without (gray bars) or with (black bars) TGFβ1. (C) Mitral VEC clones were treated ± TGFβ1 (1 ng/mL) and ± CD45 PTPase (0.5 μM) for 4 days. mRNA levels of αSMA (black), Slug (blue), MMP2 (orange), NFATc1 (teal), collagen 1 (yellow), collagen 3 (gray), TGFβ1 (red), TGFβ2 (green) and TGFβ3 (light blue) were measured by qPCR. Closed symbols indicate p values between control and

TGFβ1 treatment groups; open symbols indicate p values between TGFβ1 and TGFβ1 + CD45 PTPase inhibitor treatment groups. (D) CAECs were analyzed as in Panel C.

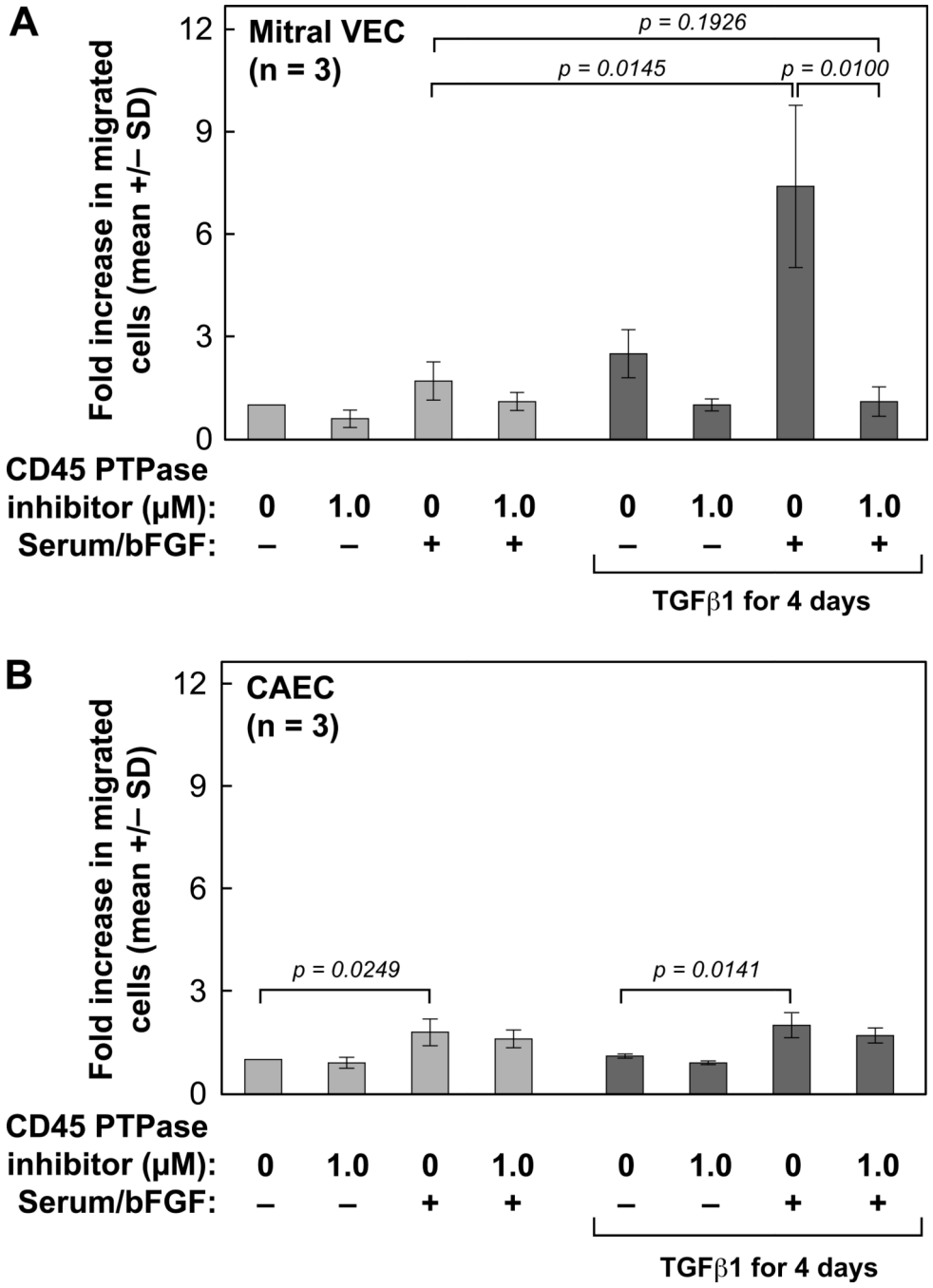

Figure 5. Increased EndMT migration blocked by CD45 PTPase inhibitor

(A) Mitral VECs were treated without (light gray bars) or with TGFβ1 (1 ng/mL) for 4 days (dark gray bars) to induce EndMT. Cells were treated ± CD45 PTPase (1.0 μM) for 30 minutes prior to and during the migration assay, as indicated. Cells were allowed to migrate across Transwell membranes towards either endothelial basal media alone or endothelial basal media + serum and bFGF for 6 hours. (B) CAEC were analyzed as in Panel A.

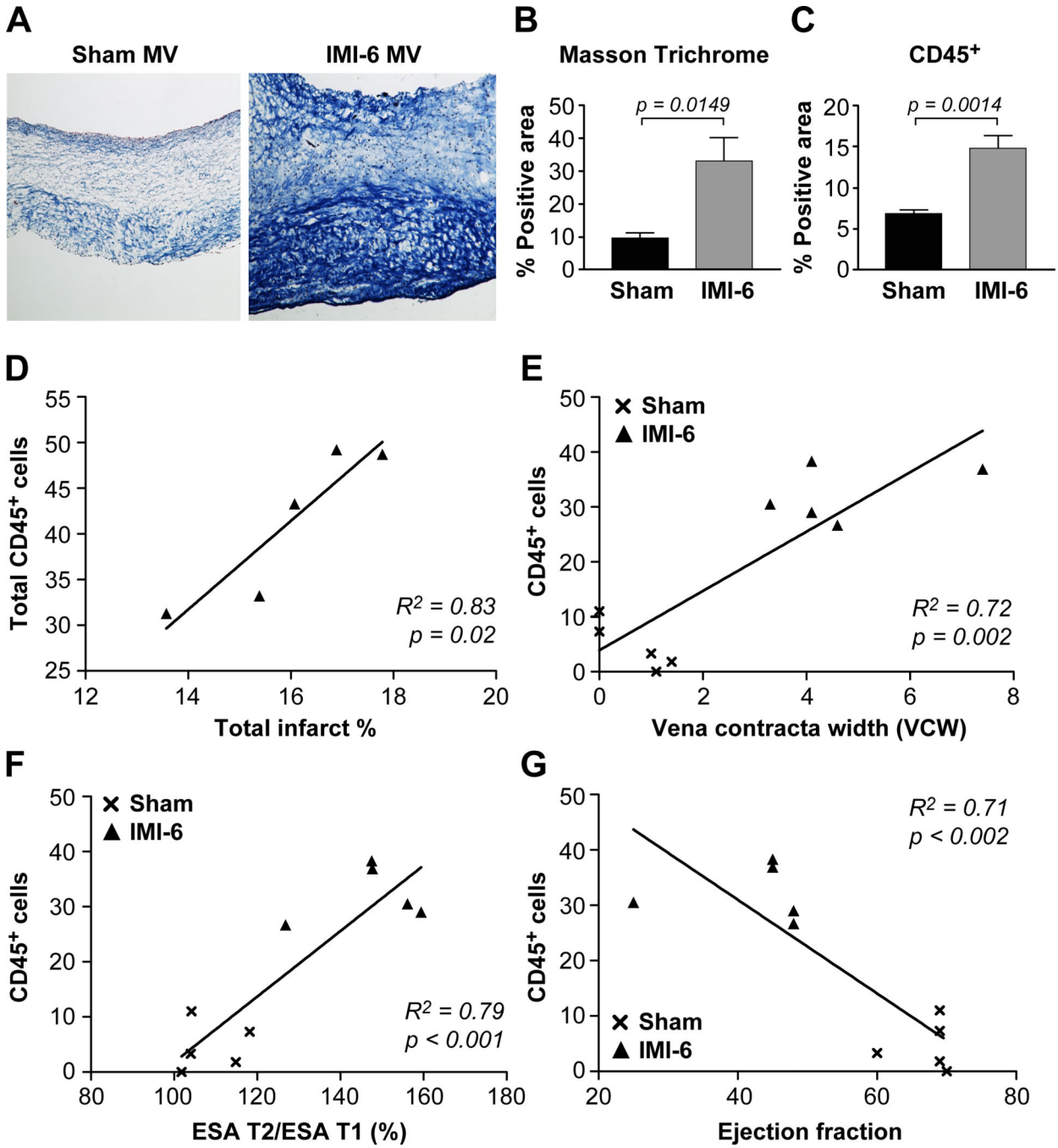

Figure 6. Fibrosis, MR severity, infarct size and LV remodeling correlate with CD45+ cells

(A) Representative images of Masson Trichrome-stained MV leaflets from sham (n=5) and IMI-6 month sheep. (B) Quantification of positively stained areas of collagen (Masson Trichrome) and (C) anti-CD45 in adjacent sections. Data were analyzed by Student's t-test using GraphPad Prism v7.0; $p<0.05$ considered significant. (D) Total CD45+ cells, measured by flow cytometry, in individual IMI-6 month sheep were plotted against infarct size (normalizing for heart size as infarct relative to total LV endocardial surface area). (E) MR was determined by measuring the width of the proximal jet (vena contracta) in the apical

long-axis view. Values for individual sheep in sham (×) and IMI-6 (▲) groups were plotted against CD45+ cells (VE-cadherin+/CD45+/αSMA+, VE-cadherin+/CD45+/αSMA-, and VE-cadherin-/CD45+/αSMA+). (F) LV remodeling, determined by the ratio of infarct endocardial surface area (ESA) at time of sacrifice (T2) / ESA at 30 minutes post-MI (T1), was plotted against the same CD45+ cells as in E. (G) Ejection fraction plotted against the same CD45+ cells as E and F. D-G, Linear regression analysis was performed and the R^2 value was calculated to see how well the regression line fit the data. $P < 0.05$ was considered significant.

Table 1

Endothelial, interstitial and hematopoietic cell populations in MVs from IMI infarcted sheep versus sham operated sheep, percentage of total cells within each cell population. Fisher test used determine variances; equal variances were found for each comparison group. Statistical significance measured using student t-test analysis. P<0.05 considered significant Comparisons with P<0.05 are shaded beige.

	Sham ***n = 5***	**6 months IMI** ***n = 5***	**Statistical Significance**
VEC VE-Cadherin^{+}/CD45^{-}/αSMA^{-}	13.5 ± 7.0	4.6 ± 6.6	*P = 0.073*
VEC^{CD45+} VE-Cadherin^{+}/CD45^{+}/αSMA^{-}	2.56 ± 2.4	9.0 ± 5.1	*P = 0.033*
VEC-EndMT VE-Cadherin^{+}/CD45^{-}/αSMA^{+}	3.1 ± 2.4	3.8 ± 3.6	*P = 0.70*
VEC^{CD45+}-EndMT VE-Cadherin^{+}/CD45^{+}/αSMA^{+}	1.18 ± 2.2	17.4 ± 4.6	*P = 0.0001*
Quiescent VIC VE-Cadherin^{-}/CD45^{-}/αSMA^{-}	65.3 ± 13.6	47.1 ± 12.8	*P = 0.060*
Activated VIC VE-Cadherin^{-}/CD45^{-}/αSMA^{+}	8.4 ± 8.7	5.3 ± 5.1	*P = 0.521*
Hematopoietic cells VE-Cadherin^{-}/CD45^{+}/αSMA^{-}	5.47 ± 3.9	8.8 ± 6.0	*P = 0.323*
Fibrocytes VE-Cadherin^{-}/CD45^{+}/αSMA^{+}	0.94 ± 2.0	5.8 ± 2.9	*P = 0.015*